Rotordynamic Forces on Centrifugal Pump Impellers

R. Franz, N. Arndt, T.K. Caughey, C.E. Brennen, and A.J. Acosta
California Institute of Technology
Pasadena, CA. 91125 USA

ABSTRACT

The asymmetric flow around an impeller in a volute exerts a force upon the impeller. To study the rotordynamic force on an impeller which is vibrating around its machine axis of rotation, the impeller, mounted on a dynamometer, is made to whirl in a circular orbit within the volute. The measured force is expressed as the sum of a steady radial force and an unsteady force due to the eccentric motion of the impeller. These forces were measured in separate tests on a centrifugal pump with radially increased shroud clearance, a two-dimensional impeller, and an impeller with an inducer, the impeller of the HPOTP (High Pressure Oxygen Turbopump) of the SSME (Space Shuttle Main Engine). In each case, a destabilizing force was observed over a region of positive whirl.

NOMENCLATURE

$[A]$	hydrodynamic force matrix, non-dimensionalized by $\rho\pi\omega^2 r_2^2 b_2$
A_2	impeller outlet area ($2\pi r_2 b_2$)
b_2	impeller discharge width
F_1, F_2	components of the instantaneous lateral force on the impeller in the rotating dynamometer reference frame
F_x, F_y	components of the instantaneous lateral force on the impeller in the fixed laboratory frame, non-dimensionalized by $\rho\pi\omega^2 r_2^3 b_2$
F_{ox}, F_{oy}	values of F_x and F_y if the impeller was at the origin of the laboratory frame (volute center), non-dimensionalized by $\rho\pi\omega^2 r_2^3 b_2$
F_n, F_t	components of the lateral force on the impeller normal to and tangential to the whirl orbit, averaged over the orbit, non-dimensionalized by $\rho\pi\omega^2 r_2^2 b_2 \varepsilon$
I/J	ratio of whirl/impeller shaft speeds
Q	flow rate
r_2	impeller discharge radius
t	time
x, y	instantaneous coordinates of the impeller center in the fixed laboratory frame, non-dimensionalized by r_2
ε	radius of the circular whirl orbit (1.3 mm)
θ	angular position of the impeller on the whirl orbit, measured from the volute tongue in the direction of impeller rotation
ρ	density of water
ϕ	flow coefficient based on the impeller discharge area and tip speed, $\frac{Q}{\omega r_2 A_2}$
ω	radian frequency of the impeller (shaft) rotation
Ω	radian frequency of the whirl motion = $I\omega/J$
HPOTP	High Pressure Oxygen Turbopump
SSME	Space Shuttle Main Engine

Figure 1. Schematic representation of the lateral forces in the rotating dynamometer frame (as F_1,F_2), in the stationary volute frame (as F_x,F_y) and in the local polar coordinate frame (as F_n,F_t).

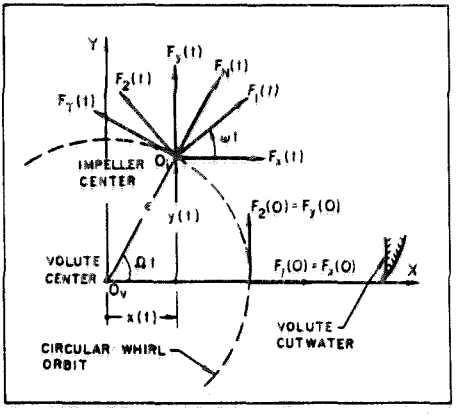

Figure 2. Assembly drawing of impeller X in the modified test section, with the inlet flange shortened.

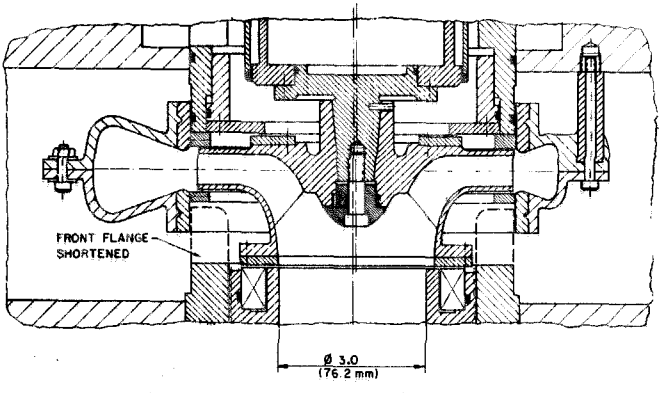

Figure 3. Assembly drawing of impeller Z installed in the test section.

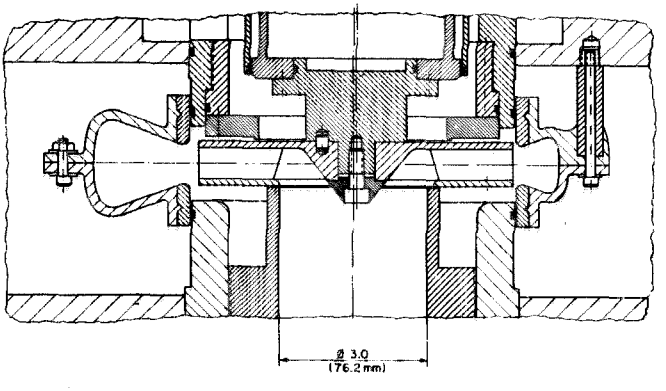

INTRODUCTION

The force experienced by a rotating turbomachine has an unsteady component related to the lateral vibration of the rotor. Knowledge of the unsteady force is crucial to understanding the rotordynamics of the turbomachine. This force has been measured on pump impellers by various authors: Jery [1-2], Ohashi [3-4] and Bolleter [5]. Presented in this paper are results for a centrifugal pump with an enlarged annular region surrounding the shroud, a two dimensional impeller and also of one half of the double-suction impeller of the HPOTP (High Pressure Oxygen Turbopump) of the SSME (Space Shuttle Main Engine).

EXPERIMENTAL FACILITY

The references [1-2] provide a description of the facility prior to the current modifications. Briefly, the dynamometer, composed of two parallel plates connected by four strain-gaged posts, is mounted between the impeller and the drive shaft. The impeller is made to whirl in an orbit about the volute center, in addition to the normal shaft rotation.

Refering to Fig. 1 the lateral force on the impeller, in the stationary volute frame of reference, can be represented by

$$\begin{Bmatrix} F_x \\ F_y \end{Bmatrix} = \begin{Bmatrix} F_{ox} \\ F_{oy} \end{Bmatrix} + [A\ (\Omega/\omega)] \begin{Bmatrix} \varepsilon/r_2\ \cos\Omega t \\ \varepsilon/r_2\ \sin\Omega t \end{Bmatrix} \qquad (1)$$

This force can be considered as the sum of two forces: a fixed force, represented by F_{ox} and F_{oy}, which the impeller would experience if located at the volute center, and an unsteady force due to the eccentric motion of the impeller, represented by a force matrix [A]. The gravitational and bouyancy forces on the rotor are subtracted out. Dimensionless quantities are used throughout (see Nomenclature for definitions).

EXPERIMENTS AND RESULTS

The forces on a five bladed Byron-Jackson centrifugal impeller, designated impeller X, in various vaneless and vaned diffusers, among them a spiral volute (volute A), were measured using the dynamometer [1-2].

Subsequently with the impeller at fixed positions on its whirl orbit, pressure measurements were taken at the volute entrance and in the annular region around the front shroud. Based on these measurements, the computation of the hydrodynamic force matrix [A] corresponding to a whirl ratio of zero had a significant contribution from the front shroud, Adkins [6-7]. During this program, the inlet flange of the test section was shortened, exposing the annular region to the housing reservoir, as shown in Fig. 2. The forces on impeller X were measured and partially reported [6-7]. During these tests, rings were installed within the volute with an axial clearance of .13 mm from the impeller to reduce leakage flow from the volute to the impeller inlet.

Impeller Z, a two-dimensional model of impeller X with logarithmic blades and a blade angle of 25°, was tested in volute A with the test section modified to eliminate the annular region, Fig. 3. Throughout these tests, the face seal clearances at the front and back of the impeller were .13 mm.

The steady force (F_o) as a function of flow coefficient is plotted in Fig. 4. Included are previous results of impeller X in volute A without

Figure 4. The magnitude and direction of the steady force $\{F_o\}$ as a function of flow coefficient at 1000 RPM of impeller X in volute A, with and without the front flange shortened, of impeller Z in volute A and of impeller R in volute E.

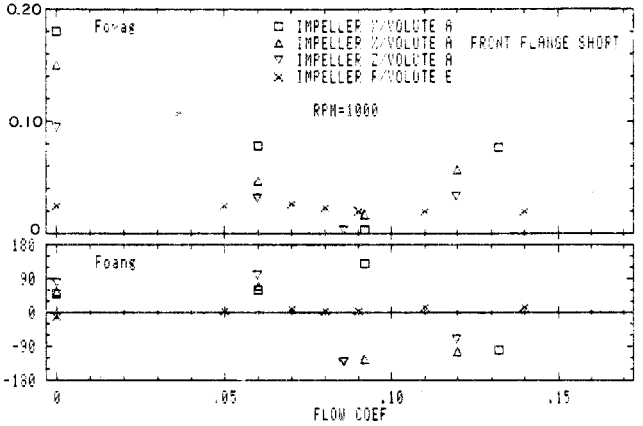

Figure 5. Average normal force at 1000 RPM with a flow coefficient of 0.06 of impeller x in volute A with and without the front flange shortened and of impeller Z in volute A.

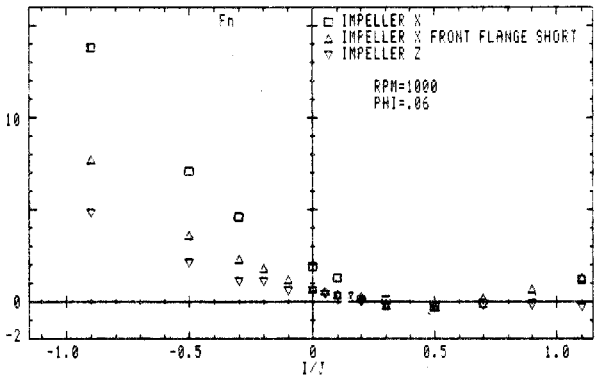

Figure 6. Average tangential force at 1000 RPM with a flow coefficient of 0.06 of impeller X in volute A with and without the front flange shortened and of impeller Z in volute A.

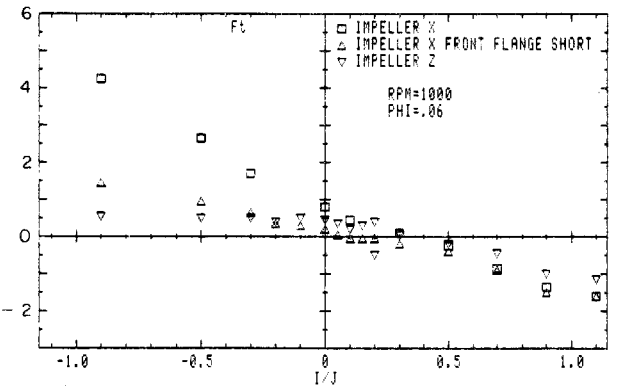

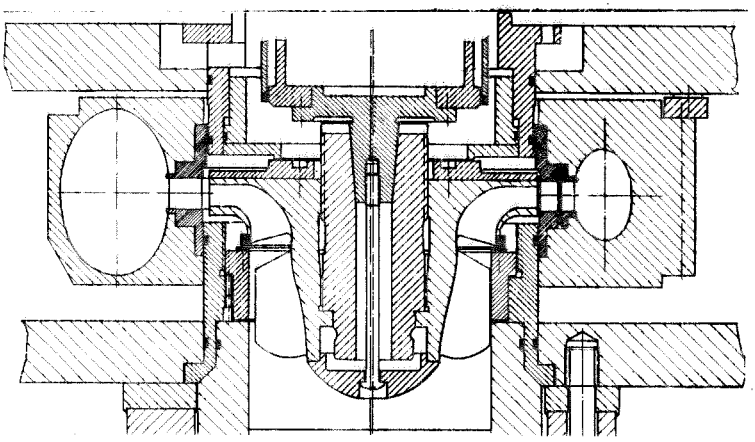

Figure 7. Assembly drawing of impeller R installed in the test section.

Figure 8. Average normal force at 1000 RPM of impeller R in volute E for various flow coefficients.

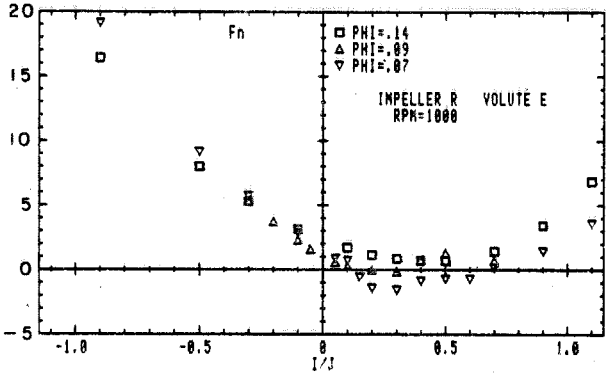

Figure 9. Average tangential force at 1000 RPM of impeller R in volute E for various flow coefficients.

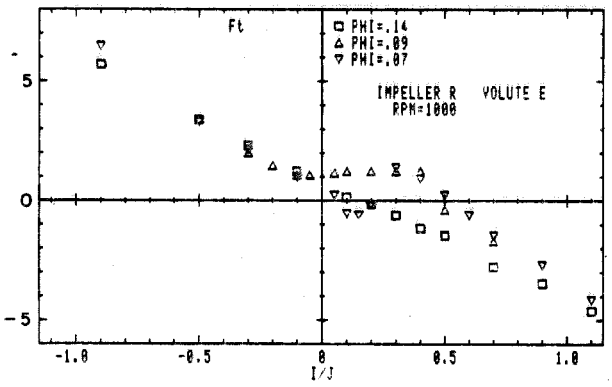

the front flange shortened. Measurements of impeller R in volute E will be discussed later. The impeller dimensions used to non-dimensionalize the forces are listed in table 1. For impeller X the force magnitude is smaller when the front flange is shortened. Impeller Z has a smaller magnitude. $\{F_o\}$ has a minimum for both impellers in the vaneless volute A.

The diagonal elements of the hydrodynamic force matrix $[A(\Omega/\omega)]$ are nearly equal and the off-diagonal elements are nearly equal but of opposite sign. The matrix will be presented in terms of the average normal and tangential forces, F_n and F_t, given by

$$F_n = (A_{xx} + A_{yy})/2 \quad \text{and} \quad F_t = (-A_{xy} + A_{yx})/2 \tag{2}$$

F_n and F_t for the two impellers are presented in Fig. 5-6 for a flow coefficient of 0.06. Under reverse whirl both F_n and F_t for impeller X are smaller with the front flange shortened. Under forward whirl F_t is in the same direction as the whirl motion, thus destabilizing, over a smaller range of whirl ratio. The forces on impeller Z are smaller. Observe that the projected area of impeller Z in the radial direction, upon which a pressure unbalance gives a lateral force, is smaller.

One half of the double-suction impeller of the HPOTP of the SSME, designated as impeller R, was installed in volute E. The impeller has eight blades and an inducer with four blades. It was modified prior to installation, principally the outlet diameter was reduced slightly. Volute E has seventeen, circular arc vanes and an elliptical cross section. Fig. 7 shows impeller R installed in volute E.

The steady force for impeller R was included in Fig. 4. There is a small variation with flow coefficient. F_n and F_t are presented in Fig. 8-9. For $\phi = 0.14$ the curve of F_n has a parabolic shape and F_t can be approximated by a straight line, with the region of destabilizing whirl $0 < \Omega/\omega < 0.2$. For $\phi = 0.09$ F_t is approximately constant over a whirl ratio of $-0.1 < \Omega/\omega < 0.4$, while for $\phi = 0.07$ F_t resembles a cubic function. Since F_t crosses the axis three times, there exit regions of stabilizing and destabilizing whirl for $0.0 < \Omega/\omega < 0.6$. At these lower flow coefficients, F_n has departed from a smooth parabola over this whirl ratio range. Reports [8-9] present the above data for more flow coefficients.

Tufts were placed upstream of the inducer, in order to make observations on flow reversal. At a position of 5 mm upstream of the inducer leading edge, flow reversal was observed for $\phi < 0.095$. For $\phi < 0.075$ flow reversal was observed in a region extending to one inducer diameter upstream of the inducer leading edge.

CONCLUSION

Exposing the annular region surrounding the shroud to the housing reservoir reduced the forces upon impeller X and reduced the destabilizing whirl ratio range of the average tangential force. These results indicate the importance of the external shroud region upon the impeller forces.

Impeller Z, a two-dimensional model of impeller X, had a smaller steady force and a hydrodynamic force matrix with smaller elements. The average tangential force was destabilizing over a whirl ratio range comparable to impeller X in the unmodified test section.

Impeller R, one half of the double-suction impeller of the HPOTP of the SSME, had the largest magnitude of the average tangential force in the region of destabilizing whirl. With decreasing flow coefficient, the curve of F_t changed from an approximately straight line to a cubic, with a

corresponding increase in the region of destablizing whirl from $\Omega/\omega < 0.2$ to $\Omega/\omega < 0.6$. This transition in the curve of F_t appears to coincide with the occurrence of flow reversal upstream of the inducer.

ACKNOWLEDGEMENTS

The authors are indebted to the NASA George Marshall Space Flight Center for continued sponsorship of this research under contract NAS8-33108.

REFERENCES

1. Jery, B., Brennen, C.E., Caughey, T.K., and Acosta, A.J., "Forces on Centrifugal Pump Impellers," "Second International Pump Symposium," Houston Texas, April 29-May 2, 1985.

2. Jery, B., "Experimental Study of Unsteady Hydrodynamic Force Matrices on Whirling Centrifugal Pump Impellers," Ph.D. Thesis, Division of Engineering and Applied Science, California Institute of Technology, 1987.

3. Ohashi, H., and Shoji, H., "Lateral Fluid Forces Acting on a Whirling Centrifugal Impeller in Vaneless and Vaned Diffuser," Workshop on Rotordynamic Instability Problems in High Performance Turbomachinery, Texas A&M University, May 1984, NASA CP-2338, pp. 109-122.

4. Ohashi, H., Hatanaka, R., and Sakurai, A., "Fluid Force Testing Machine for Whirling Centrifugal Impeller," International Conference on Rotordynamics, Tokyo, Japan, Sept. 14-17, 1986.

5. Bolleter, U., Wyss, A., Welte, I., and Stürchler, R., "Measurement of Hydrodynamic Interaction Matrices of Boiler Feed Pump Impellers," ASME 85-DET-148, 1985.

6. Adkins, D., "Analyses of Hydrodynamic Forces on Centrifugal Pump Impellers," Ph.D. Thesis, Division of Engineering and Applied Science, California Institute of Technology, 1986.

7. Adkins, D., Brennen, C.E., "Analyses of Hydrodynamic Radial Forces on Centrifugal Pump," Fourth Rotordynamic Instability Problems in High Performance Turbomachinery Workshop, Houston, Texas, June 2-4, 1986.

8. Franz, R. and Arndt, N., "Measurements of Hydrodynamic Forces on a Two-Dimensional Impeller and a Modified Centrifugal Pump," Division of Engineering and Applied Science, California Institute of Technology, 1986, Report No. E249.4.

9. Franz, R. and Arndt, N., "Measurements of Hydrodynamic Forces on the Impeller of the HPOTP of the SSME," Division of Engineering and Applied Science, California Institute of Technology, 1986, Report No. 249.2.

LIST OF TABLES

Table 1. Impeller Dimensions

Impeller	r_2 (mm)	b_2 (mm)
X	81.0	15.7
Z	81.0	15.7
R	83.8	14.5